

Evaluation of Stress Environment around Pits in Nickel Aluminum Bronze Metal under Corrosion and Cyclic Stresses

Ramana M. Pidaparti¹ and Alex C. Johnson¹

Abstract: Surface damage in the form of pitting was observed in NiAl Bronze metal subjected to corrosion and cyclic stresses. In order to investigate the stresses surrounding the evolving pits due to corrosion, an image based computational study was carried out. The computational study involves developing an analysis model from the SEM images of corroded pits and then conducting stress analysis. Several computational simulations were carried out with increasing/evolving pits and the corresponding stress environment was obtained. The results obtained indicate that pit profiles (size and height) greatly affect the stress environment and the maximum stresses may vary depending on the pit profile. Overall, the results obtained illustrate that the stress environments around pit profiles are non-uniform and can attain maximum values at various locations around the pits due to non-uniformity of pit profiles in NAB metal. From these stresses, it is possible to predict where the cracks (Mode I and Mode II) or mixed mode (Mode I & II) may initiate from the pit profiles in the material.

Keywords: NAB metal, Pits, Stresses, Corrosion, SEM, Image Analysis

1 Introduction

Engineering components made from nickel aluminum bronze (NAB) metal is being used in the Navy's ship and propeller components due to their high toughness. However, this metal is subjected to pits and stress corrosion cracking due to operating in a salt water environment. In order to reduce the maintenance requirements, expedite repair, and extend the life of naval nickel aluminum bronze components, engineering studies are being carried out to investigate the mechanism of stress corrosion crack initiation through experiments and modeling.

¹ Department of Mechanical Engineering, Virginia Commonwealth University, 401 West Main Street, Richmond, VA 23284

Pitting and stress corrosion cracking are known to be some of the major damage mechanisms affecting the integrity of NAB materials and structures in nuclear and naval engineering. Corrosion pits generally initiate due to some chemical or physical heterogeneity at the surface, such as inclusions, second phase particles, flaws, mechanical damage, or dislocations. Many NAB alloys contain numerous constituent particles, which play an important role in corrosion pit formation [Vasanth and Hays (2004); Dersch and Cohn (2001); Fuller et al (2007); Wharton et al (2005); Oh-Ishi and McNelley (2004)]. To better understand particle-induced pitting corrosion, optical microscopy, Scanning Electron Microscopy (SEM) and Transmission Electron Microscopy (TEM) techniques have been used. Due to operating and special service environments (e.g. saltwater), corrosion pits and stress corrosion cracking are readily formed between the constituent particles and the surrounding matrix in these alloys [Oh-Ishi and McNelley (2004)].

Micro-cracks usually initiate from the corrosion pit sites in the material. Under the interaction of cyclic load and the corrosive environment, cyclic loading facilitates the pitting process, and corrosion pits, acting as geometrical discontinuities, lead to crack initiation and propagation and then final failure [Burstein et al (2004); Rokhlin et al (1999); Ishihara et al (2006); Sriraman and Pidaparti (2009)]. Corrosion can lead to accelerated failure of structural components under fatigue loading conditions. Understanding and predicting corrosion damage morphology in the form of pits/cracks is therefore very important for the structural integrity of materials and structures. Electrochemical probe techniques such as Scanning Reference Electrode Technique (SRET), Scanning Vibrating Electrode Technique (SVET), and Localized Impedance Spectroscopy (LEIS) [Isaacs (1988); Suter and Bohni (1997); Oltra and Vignal (2007); Paik and Alkire (2001)] have been used for electrochemical measurements at the metal surface. There are no probe related techniques that quantitatively assess the corrosion morphology in the form of pits and stress corrosion cracking in metals. Recently, Pidaparti et al. [Pidaparti and Patel (2008); Pidaparti et al (2009); Pidaparti and Patel (2011)] developed a computational methodology to predict stresses around pits and found that pit induced stresses reach a plateau after a certain period of corrosion time. They also showed that pits may lead to crack initiation, and that this phenomena changes with the corrosion environment.

Recently, Pidaparti et al. [Pidaparti et al (2010)] used image analysis to characterize defects in NAB metal. However, they didn't investigate the defect induced stresses in NAB metals. In order to qualitatively and quantitatively characterize the early stage damage mechanisms in NAB metals under corrosion and cyclic stresses, image based stress analysis of corrosion pit morphology may be used as a tool to predict the nucleation of cracks resulting from initiation and growth of pits. In

this study, image based stress analysis was used to investigate the stress environment around pit profiles observed in Nickel Aluminum Bronze metal under varying corrosion conditions and applied cyclic stresses.

2 Experimental Data

Nickel Aluminum Bronze alloy metal samples were cut into 50 mm X 5 mm X 1mm dimensions from a plate. The weight percentage chemical composition of the NAB plate [Vasanth and Hays (2004)] is 8.7%-9.5% Al; 4.0%-4.8% Ni; 3.5%-4.3% Fe; 1.2%-2.0% Mn; 0.1% Si; 0.02% Pb and the rest is Cu with average tensile strength of 731 MPa and Rockwell B Hardness of 203 (HRB). The NAB plate's typical microstructure consists of continuous equiaxed crystals with small areas of metastable β phases. γ phase precipitates are found at grain boundaries in α phase and β phases areas [Vasanth and Hays (2004)]. Initially, the specimens were first inspected visually and diamond polished up to a surface finish of 3 μm before the corrosion testing. These specimens were immersed in 10% ammonia (NH_4OH) (by vol.) - 90% seawater (by vol.) prepared as per ASTM D1141 standard and the cyclic stress was applied under three point bending according to ASTM G39.

After exposing the specimens for a specific corrosion time (1 to 37 days) under specified cyclic stress (0 to 310 MPa), the samples were examined under SEM to characterize the surface morphology. The experiments were conducted by the researchers at the Department of Alloy Development and Mechanics, Carderock Division, Naval Surface Warfare Center, Bethesda, Maryland. They provided the SEM image data to VCU for further analysis. Stress analysis of the SEM data was carried out in this study. The corrosion morphology of typical NAB specimens with pits is shown in Fig. 1. These SEM images were used in the image analysis to develop features to characterize the stress environment around pits in NAB metal.

3 Stress Analysis Method

An SEM image of a corrosion pit profile was imported into a NURB modeling software, Rhinoceros to create an image-based finite element model of corrosion pits. Initially, the selected SEM images were enhanced using Gimp software, which is very similar to Photoshop. A 'Heightfield from Bitmap' command in Rhinoceros was used to generate a surface of the corrosion pit profile using the SEM image by assigning height to each color value of a bitmap image. The height of the surfaces was scaled down to match the actual pit depth from the experiment. The surfaces were then imported into the CAD modeling software, SolidWorks to create a 3D model of the corrosion pits by specifying the thickness/height. The 'Extrude' command was used to create a non-corroded portion of the specimen. This 3D model

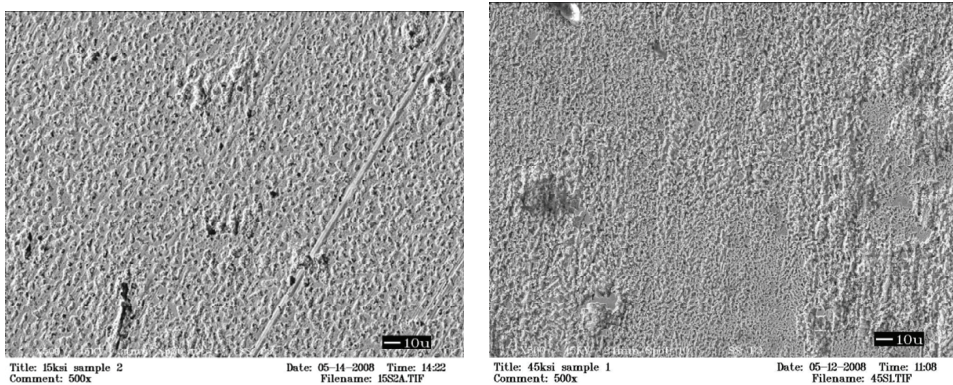


Figure 1: Typical pit surface morphologies of corroded NAB specimens

was then imported into finite element analysis software, ANSYS for stress analysis. This procedure is similar to the analysis carried out on aluminum specimens [?].

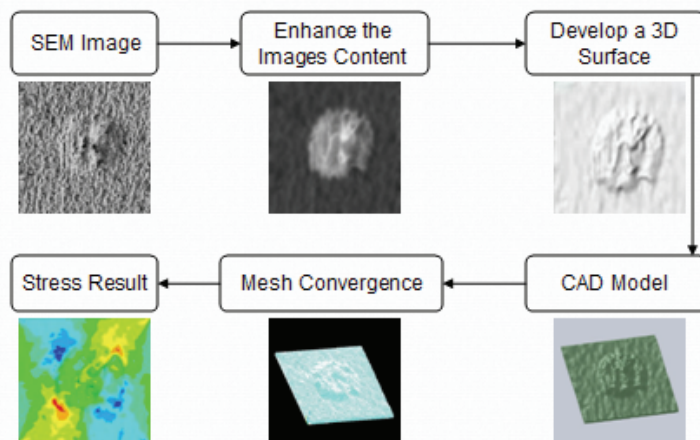


Figure 2: An overview of the computational process for stress estimation around pits

Figure 2 shows a flow chart of procedures used to create the SEM-based finite element model. Solid brick elements were used to represent the model and the convergence test was performed on the finite element model with a global element size of 9×10^{-7} mm, which provided consistent results for stress. Linear elastic material model of the pure NAB alloy with Young's modulus ($E = 110$ GPa) and

Poisson's ratio ($\nu = 0.32$) was used in the analysis. Fixed-displacement boundary conditions were applied to four bottom corners and uniform pressure of 1 Pa was applied to the bottom surface. The converged finite element models for the each of samples include, sample #1 - 86,439 elements, sample #2 - 78074 elements, sample #3 - 103279 elements, sample #4 - 64088 elements and sample #5 - 155290 elements. Simulations were carried out for all five samples to investigate the effect of pit sizes on von-Mises stress and in-plane shear stresses.

4 Results and Discussion

Typical surface pit morphologies under corrosion and cyclic stresses obtained from the testing are shown in Fig. 1. It can be seen from Fig. 1 that the scanning electron micrographs (SEM) show pits scattered around the specimen surfaces. After considering a number of such micrographs, five different pit sizes were selected for the analysis. The pit sizes and their heights, as well as their 3D profiles for the five specimens are shown in Fig. 3. It can be seen from Fig. 3 that the single pit size increases both in size as well as height for the five specimens considered. Figure 4 shows the typical finite element model for a sample and the boundary conditions.

Figure 5 shows the von-Mises stress distributions over the five samples for the different pit sizes considered. It can be seen from Fig. 5 that stress distribution is non-uniform and focused more around pit valleys. The maximum stress location varies from sample to sample with varying pit sizes and profiles. Overall the results of stress distributions in Fig. 5 reflect that pit profiles greatly affect the stress distribution around the pits environment. The maximum von-Mises stress is plotted with pit size/profile for all the samples considered in Fig. 6. It can be seen from Fig. 6 that maximum von-Mises stress of 17.2 MPa was obtained for sample #4 with a pit height of 8 μm . Similarly, a minimum von-Mises stress of 7.38 MPa was obtained for sample #5 with a pit height of 10 μm but of larger size pit. There is no specific trend in von-Mises stress with increasing pit height due to overall pit profile and size. The in-plane shear for all the five samples is given in Fig. 7. The in-plane shear stress increases by about 291% when the pit height is increased about 3 times as seen from Fig. 7. Further increase in pit height decreases the stress by 83% and this is due to large size of the pit and the profile. Both maximum von-Mises stress and in-plane shear stress play an important role in damage development from pits. Usually, the maximum von-Mises stress happens to be tensile which will be very critical as these type of stresses are responsible for Mode I type of crack, which in turn makes more damage and further damage development. In contrast, the in-plane shear stresses which are responsible for the development of Mode II cracks that are not as severe as Mode I crack. In general, the crack development from pits depends on the pit morphology as well as the orientation of loading acting on the

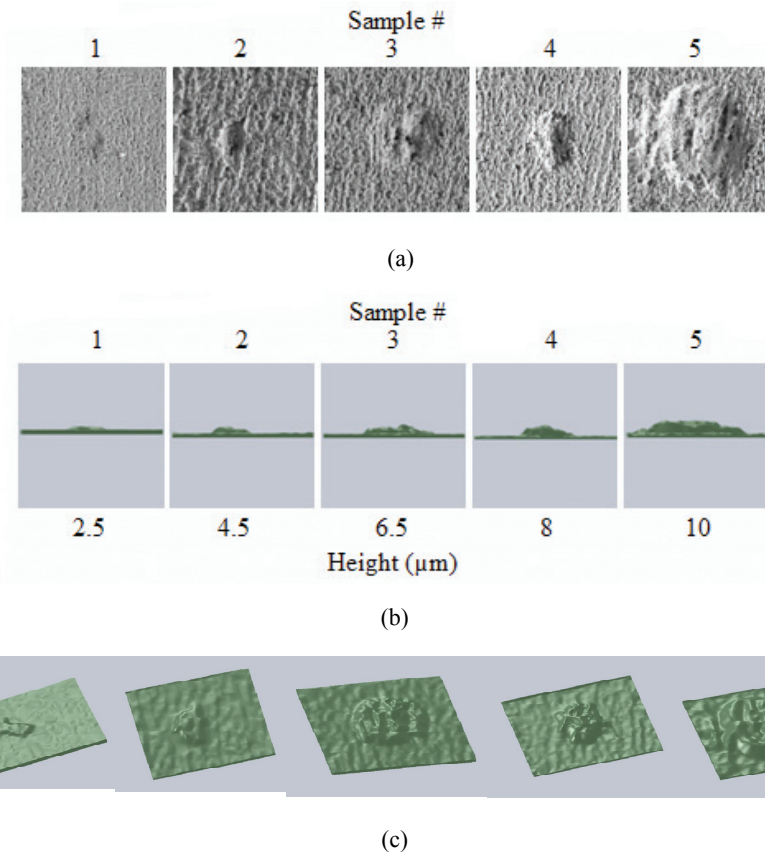


Figure 3: Samples of pit profiles with increasing size (a) and their height (b) and 3D profiles (c)

material/structure [Xiao-Guang and Jin-Quan (2012); Turnbull et al (2010)].

Overall, the results presented in Figs. 5-7 illustrate that the stress environment around pit profiles are non-uniform and can attain a maximum values at various locations around the pits due to non-uniformity of pits. From these stresses, it is possible to predict where the cracks (Mode I and Mode II) or mixed mode (Mode I & II) may initiate from the pit profiles in the material.

5 Conclusions

An image based computational stress analysis was used to study the pit profile morphology of Nickel Aluminum Bronze metal under varying corrosion conditions and applied cyclic stresses. Several pit profiles were selected from SEM images and

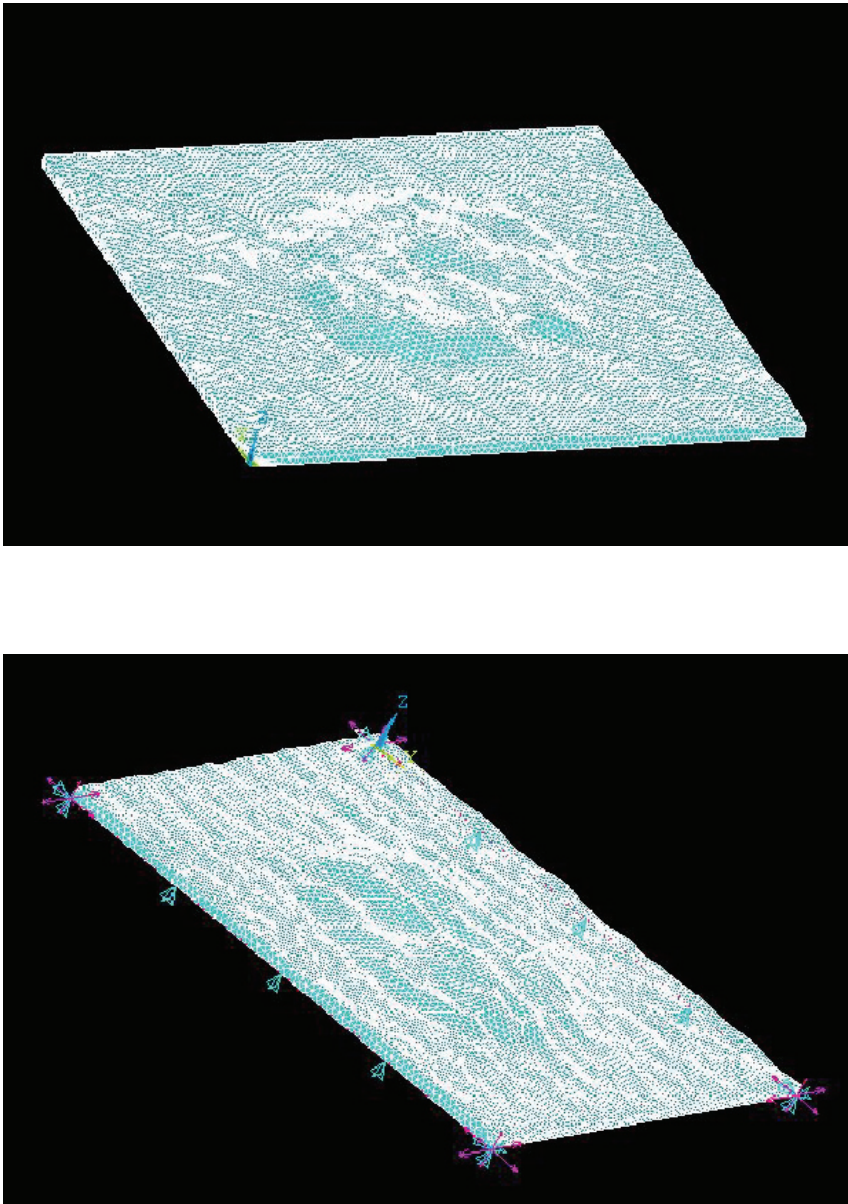


Figure 4: Typical finite element model (top) and boundary conditions (bottom) for samples of pit profiles shown in Fig. 3(c)

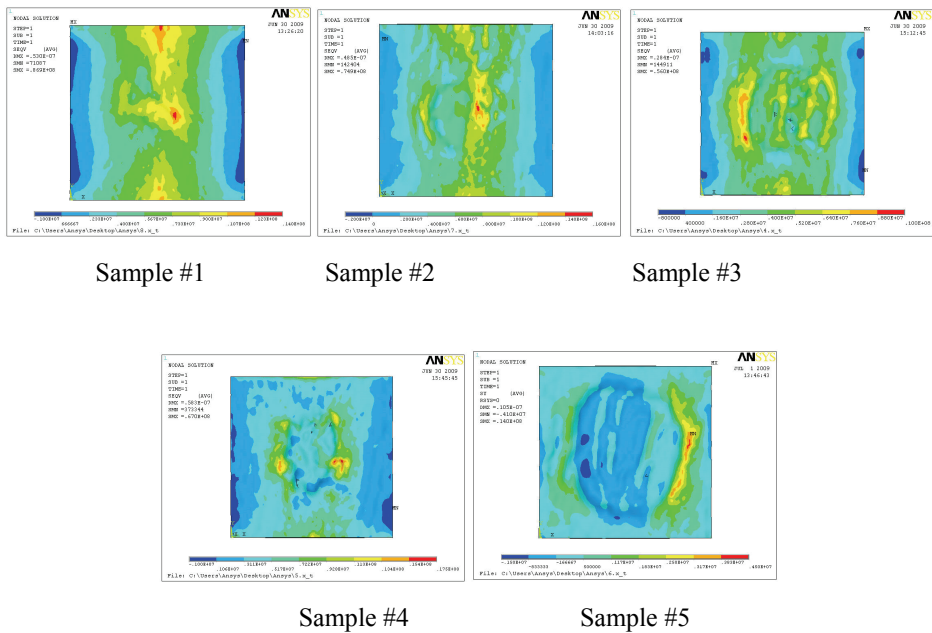


Figure 5: Distribution of von-Mises stress around pit profiles considered in various samples

a computational stress analysis was carried out to investigate the stresses around pit profiles. The results obtained from stress analysis indicate that pit profiles (size and height) greatly affect the stress environment and the maximum stresses may vary depends on the pit profile. Overall, the results obtained illustrate that the stress environment around pit profiles are non-uniform and can attain a maximum values at various locations around the pits due to non-uniformity of pit profiles. From these stresses, it is possible to predict where the cracks (Mode I and Mode II) or mixed mode (Mode I & II) may initiate from the pit profiles in the material. However, more research is needed to study further the proposed methods/analysis based on SEM images.

Acknowledgement: The authors thank US National Science Foundation for supporting this work through a grant DMR-0505496, and supporting Alex Johnson through NSF-REU program. The authors also acknowledge the technical support, especially the experimental data used in this study from Ms. Angela Whitfield, Drs. Rao and Mercier of the Department of Alloy Development and Mechanics, Carderock Division, Naval Surface Warfare Center, Bethesda, Maryland. The authors

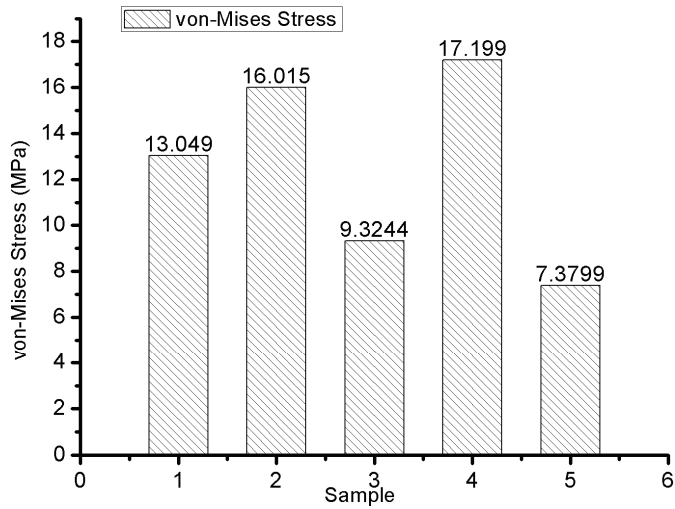


Figure 6: Von-Mises stress variation with increasing pit sizes for the five samples considered

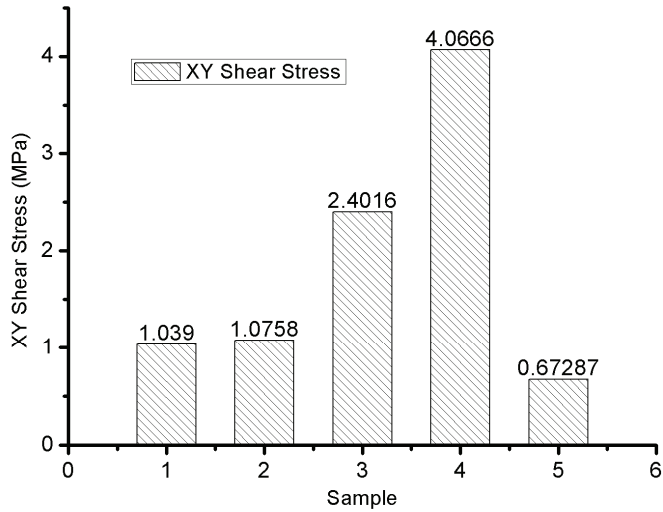


Figure 7: In-plane shear stress variation with increasing pit sizes for the five samples considered

also acknowledge the financial support from Dr. Airan Perez, Program Officer, Office of Naval Research, Virginia.

References

Burstein G. T., Liu C., Souto R. M., Vines S. P. (2004): Origins of Pitting Corrosion, Corrosion Engineering, *Science and Technology* 39, 25.

Dersch F. M., Cohn A. (2001): Ultrasonic Inspection of Nickel Aluminum Bronze for Stress Corrosion Cracking, NSWCCD-61-TR-2001-21.

Fuller M. D., Swaminathan S., Zhilyaev A. P., McNelley T. R. (2007): Microstructural Transformations and Mechanical Properties of Cast NiAl Bronze: Effects of Fusion Welding and Friction Stir Processing, *Materials Science and Engineering*, 463 (1-2), 128-137.

Isaacs H. S. (1988): Initiation of stress corrosion cracking of sensitized type 304 stainless steel in ductile thiosulfate solution, *Journal of the Electrochemical Society* 135, 2180-2183.

Ishihara S., Saka S., Nan Z. Y., Goshima T., Sunada S. (2006): Prediction of corrosion fatigue lives of aluminum alloy on the basis of corrosion pit growth law, *Fatigue Fract Engng Mater Struct* 29, 472-480.

Oh-Ishi K., McNelley T. R. T. R. (2004): Microstructural Modification of As-Cast NiAl Bronze by Friction Stir Processing, *Metallurgical and Materials Transactions* 35, 2951-2961.

Oltra R., Vignal V. (2007): Recent advances in local probe techniques in corrosion research – Analysis of the role of stress on pitting sensitivity, *Corrosion Science* 49, 158-165.

Paik C. H., Alkire R. C. (2001): Role of sulfide inclusions on localized corrosion of Ni200 in NaCl solutions, *Journal of the Electrochemical Society* 148, 276-281.

Pidaparti R. M., Patel R. R. (2008): Correlation between Corrosion Pits and Stresses in Al Alloys, *Journal of Materials Letters* 62, 4497-4499.

Pidaparti R. M., Koombua K., Rao A. S. (2009): Corrosion Pit Induced Stresses Prediction from SEM and Finite Element Analysis, *International Journal for Computational Methods in Engineering Science and Mechanics* 10, 117-123.

Pidaparti R.M., Patel R.R. (2011): Modeling the Evolution of Stresses Induced by Corrosion Damage in Metals, *Journal of Materials Engineering and Performance*, Vol. 20, No. 7, pp. 1114-1120.

Pidaparti R.M., Aghazadeh B.S., Reynolds A., Rao A. S., Mercier G. (2010): Classification of Defects in NiAl Bronze through Image Analysis, *Corrosion Science*, Vol. 52, No. 11, pp. 3661-3666.

Rokhlin S. I., Kim J. Y., Nagy H., Zoofan B. (1999): Effect of pitting corrosion on fatigue crack initiation and fatigue life, *Engng. Fract. Mech.* 2, 425-444.

Sriraman M. R., Pidaparti R. M. (2009): Life Prediction of Aircraft Aluminum subjected to Pitting Corrosion under Fatigue Conditions, *Journal of Aircraft* (7-8), 1253-1259.

Suter T., Bohni H. (1997): A new microelectrochemical method to study pit initiation on stainless steels, *Electrochimica Acta*, 42, 3275-3280.

Turnbull A., Wright L., Crocker L. (2010): New insight into the pit-to-crack transition from finite element analysis of the stress and strain distribution around a corrosion pit, *Corros. Sci.*, 52, 1492-1498.

Vasanth K. L., Hays R. A. (2004): Corrosion Assessment of Nickel-Aluminum Bronze (NAB) in Seawater, *Corrosion*, Paper No. 04294.

Wharton J. A., Barik R. C., Kear G., Wood R. J. K., Stokes K. R., Walsh F. C. (2005): The corrosion of Nickel-Aluminum Bronze in Seawater, *Corrosion Science* 47, 3336-3367.

Xiao-Guang H., Jin-Quan X. (2012): Pit morphology Characterization and Corrosion Fatigue Crack Nucleation Analysis based on Energy Principle, *Fatigue & Fracture of Engineering Materials & Structures*, (in-press)

